ISSN 0915-633X

NATIONAL INSTITUTE FOR FUSION SCIENCE

Behavior of Hydrogen Atoms in Boron Films during H_2 and He Glow Discharge and Thermal Desorption

K. Tsuzuki, M. Natsir, N. Inoue, A. Sagara, N. Noda, O. Motojima, T. Mochizuki, I. Fujita, T. Hino and T. Yamashina

(Received - Aug. 10, 1995)

NIFS-374 Sep. 1995

RESEARCH REPORT
NIFS Series

NAGOYA, JAPAN

BEHAVIOR OF HYDROGEN ATOMS IN BORON FILMS DURING H_2 AND He GLOW DISCHARGE AND THERMAL DESORPTION

K. Tsuzuki, M. Natsir, N. Inoue[1], A. Sagara[1], N. Noda[1], O. Motojima[1], T. Mochizuki[2], I. Fujita[2], T. Hino[2], and T. Yamashina[2]

The Graduate University for Advanced Studies, Furo-cho Chikusa-ku Nagoya 464-01, Japan
[1]National Institute for Fusion Science, Furo-cho Chikusa-ku Nagoya 464-01, Japan
[2]Department of Nuclear Engineering. Hokkaido University Sapporo 060, Japan

ABSTRACT

Hydrogen absorption and desorption characteristics in boron films deposited on a graphite liner have been studied. Number of hydrogen atoms absorbed in the films is estimated from a decrease in hydrogen pressure during a hydrogen glow discharge. It was 1.9×10^{17} atoms/cm^2 in the 1 hour discharge after an evacuation of H atoms contained in the original boron films by thermal desorption. Hydrogen atoms were absorbed continuously without saturation for 3 hours during the discharge. Number of H atoms absorbed reached to 2.6×10^{17} atoms/cm^2 at 3 hour. A discharge in helium was carried out to investigate H desorption characteristics from hydrogen implanted boron films. It was verified that reactivity for hydrogen absorption was recovered after the He discharge. Hydrogen atoms were accumulated in the films by repetition of alternate He and H_2 discharge. Thermal desorption experiments have been carried out by raising the liner temperature up to 500°C for films after 1 hour, 3 hours hydrogen discharge and 6 times repetition of H_2/He discharges. Most of H atoms in the films were desorbed for all these cases. The slow absorption process was confirmed through the thermal desorption experiments.

Keywords
boron coating films, hydrogen recycling, hydrogen retention, hydrogen glow discharge, helium glow discharge, thermal desorption

---

A contributed paper to be presented in 13th International Vacuum Congress in Yokohama from September 25 to 29, 1995. To be published in Vacuum.

1. INTRODUCTION

In situ boron coating (boronization) of the first wall of plasma machine has been applied to many fusion-experimental devices, and improvement of the plasma performance has been observed[1-7]. Metal impurities are reduced because the wall is coated with the low Z material. Reduction of oxygen impurity is observed[1-7] since the B films have oxygen gettering ability[8,9], which is a favorable effect for fusion devices.

The deposited boron films contain hydrogen, and absorb or desorb (recycle) the hydrogen during the plasma discharge, which makes plasma-density control difficult[1-3]. This problem will be especially important in future self-burning reactor, where fusion power is directly connected to fuel control[10]. It is reported that, at elevated temperature in JT-60U, hydrogen recycling rate is remarkably lower with a boronized wall than with a carbon wall[7]. On the other hand, in CHS, it is higher with a boronized wall at room temperature than with a titanium-flashed wall[4]. It is also reported that the energy confinement is better for lower hydrogen recycling[7]. Tritium inventory of boronized wall will be a severe problem in D-T experiments in future. Helium discharge cleaning is widely used to reduce hydrogen recycling[2-4,7], but the quantitative evaluation has not been achieved. Thus precise understanding of hydrogen behavior is very important for present and future fusion studies. However, available data so far obtained are not sufficient to understand the both H retention and recycling characteristics of the boron films.

In this experiment, hydrogen absorption with H_2 glow discharges, desorption with He discharges, and thermal desorption have been studied for B films.

2. EXPERIMENTAL

An experimental device named SUT (SUrface modification Test-stand)[9] is used for this study. A cylindrical chamber of 530mm in diameter and 500mm in height is pumped by two turbo-molecular pumps of tandem configuration, which enable the base pressure of less than 10^{-9} Torr. A graphite liner (IG-430U) of 400mm in diameter and 400mm in height is set in the chamber. A tungsten rod is inserted at the center of the liner as an anode. The liner can be heated up to 500°C by molybdenum heater in the chamber. The rest of the chamber is kept at room temperature during the heating procedure of the liner. In order to prepare boron films on the inner surface of the liner, B_2H_6 (5% in He) gas is introduced with net flow rate of 2.4sccm through a mass flow controller. Total pressure is kept 0.02Torr by controlling pumping speed with an adjustable valve. A glow discharge (0.2A, 400V) is ignited between the anode and the grounded liner. The thickness of boron films is monitored by a quartz oscillator. The coating is continued until the thickness reaches 200nm (typically 72min). Temperature of the liner increases from room temperature to 120°C during the coating process due to a power flow from the plasma. Prior to H_2 exposure, the boron film is once heated up to 500°C to evacuate the H atoms retained originally in the films during the coating.

Hydrogen absorption in the deposited boron film is measured with a diaphragm gauge during a glow discharge in hydrogen (typically 0.02Torr, 0.2A, 500V). The ion impact desorption of hydrogen is investigated by a glow discharge in helium (typically 0.02Torr, 0.2A, 350V), and the thermal desorption is also investigated by heating the liner up to 500°C. The Quadrupole Mass Spectrometer (QMS) with a

differential pumping system is used for the measurement of the hydrogen desorptions due to the He discharge and heating. The absolute sensitivity for H_2 gas is calibrated by the diaphragm gauge just before the each experiment.

3. RESULTS

3.1 H_2 glow discharges and thermal desorptions

In order to evaluate hydrogen capacity, the boron films were exposed to an H_2 glow discharge. Figure 1 shows time evolution of total pressure measured by the diaphragm gauge during the first H_2 discharge after the thermal desorption. Discharge condition was as follows, H_2 flow rate : 26sccm, pressure : 0.02Torr, discharge current : 0.2A, discharge voltage : 500V. According to gas monitoring by QMS, no significant increase in any impurities was observed during the discharge. The trace in Fig.1 corresponds to the change in hydrogen partial pressure. The H_2 pressure decreased when the discharge was ignited (Time : t= 0min). This is understood as a result of hydrogen absorption in the boronized wall. When the discharge was switched off (t=60min), the pressure once increased, and returned to the initial value before the discharge. The amount of retained H atoms was calculated by integrating the pressure drop (ΔP) with the following equation.

$$n_H = k\int \Delta p \bullet S_p dt / A \qquad (1)$$

n_H : hydrogen density (atoms/cm^2)
k : conversion factor (atoms/Torr l)
ΔP: pressure difference from the initial value (Torr)
S_p: pumping speed for H_2 (15.4l/s)
A : Area of the liner (7000cm^2)

It was $(1.9\pm0.05)\times10^{17}$ atoms/cm^2 at 1 hour. Within 30 minutes, the pressure came to a value close to the initial one. However, this pressure was clearly lower than the initial value as is seen in Fig.1. The difference was of 1.0×10^{-4} Torr at 60 min. This means that H atoms were continuously absorbed until the end of the discharge of 1 hour.

When a hydrogen discharge was continued for longer time, the pressure difference (ΔP) decreased slowly without saturation and became 5.3×10^{-5} Torr at 3 hour. The estimated H retention reached $(2.6\pm0.3)\times10^{17}$ atoms/cm^2, which was 0.7×10^{17} larger than that of the 1 hour discharge.

Thermal desorption experiments have been carried out by raising the temperature of the whole liner up to 500°C after the H_2 discharge. Figure 2 shows H partial pressure during the thermal desorption after the H_2 discharge of 1 hour (solid line), together with the liner temperature (dotted line) against time. The hydrogen pressure increased almost linearly with the liner temperature and reached a peak value at 400°C. The temperature was kept at 500°C for 30 minutes, during which the H pressure decreased continuously. The number of desorbed H atoms was calculated from eq.(1), and estimated to be $(2.05\pm0.05)\times10^{17}$

atoms/cm^2. Similar curve was obtained during the thermal desorption after the H_2 discharge for 3 hours and the H atoms of $(2.40\pm0.05)\times10^{17}$ atoms/cm^2 were desorbed.

The amount of absorbed and desorbed H atoms are shown in Figure 3 for the cases of H_2 discharge of 1 hour and 3 hours, followed by thermal desorption. The desorbed H atoms are almost equal to absorbed atoms within the experimental error in both cases. Number of the absorbed hydrogen increased when the discharge was continued for 3 hours. The result in Fig.3 confirms a long time continuing absorption process during the hydrogen discharge.

3.2 Effect of He glow discharges

A discharge in helium (0.2A, 350V) was carried out for 15 minutes after the first H_2 discharge in order to investigate the desorption behavior of H atoms by the impact of He ions. The H_2 pressure, monitored by QMS, increased when the discharge was ignited. The desorbed amount was calculated according to eq.(1) and estimated to be $(0.2\pm0.05)\times10^{17}$atoms/cm^2. Around 10% of the absorbed H atoms were desorbed.

To clarify the effect of He discharge to H_2 absorption, the second H_2 discharge was applied after the He discharge. The decrease of the pressure similar to Fig.1 was observed during the H_2 discharge. It means the surface of the boron film was activated by He discharge to absorb hydrogen. Hydrogen atoms of $(0.39\pm0.02)\times10^{17}$atoms/cm^2 were absorbed in the second H_2 discharge for 15 minutes following to the He discharge. To compare the desorbed and absorbed amounts, time variations of the pressure difference ($|\Delta P|$) are plotted in Fig.4. H atoms absorbed in the second H_2 discharge(c) was lager than those desorbed in He discharge(b). The difference corresponds to the hatched area in Fig.4. To confirm the effect of H accumulation, the alternate H_2 and He discharges were repeated for 6 times. Figure 5 shows the time variation of retained H atoms in the film estimated from ΔP. Hydrogen atoms were gradually accumulated in the film by the repetition.

After 6 times repetition of the alternate discharges, thermal desorption experiment was carried out. Hydrogen atoms of $(2.40\pm0.05)\times10^{17}$ atoms/cm^2 were desorbed. This number is 0.35×10^{17} atoms/cm^2 larger than that after the H_2 discharge of 1 hour. This difference is equal to estimated H accumulation during the repetition in Fig.5. Most of the hydrogen atoms retained in the film were desorbed by the thermal desorption experiment, in this case, too.

4. DISCUSSIONS

In the first H_2 discharge after the thermal desorption, maximum hydrogen flux into the film was 5.9×10^{14} atoms/cm^{2}sec, which corresponds to 160% of the ion flux to the film. Not only ions but also neutral atoms or radicals might be absorbed. The surface was reactive enough to capture most of ions, atoms, and radicals coming to the film. When the discharge is continued, the reactivity of the film decreased due to increase in the surface density of H atoms. At 30 minute in Fig.1, only 5% of the ion flux was absorbed, but the absorption continued as long as 3 hours as mentioned in chapter 3. This long continuing absorption might be caused by diffusion of H atoms into the film. This diffusion can be

explained if we assume a diffusion constant of at least around 10^{-15}~10^{-13} cm^2/s, which is within the reasonable value.

In the discharge in helium, only 10% of implanted H atoms were desorbed. However, in the second discharge following to the He discharge, the maximum absorption flux reached 50% of that of the first H_2 discharge as shown in Fig.4. The He ion bombardment may induce H desorption mainly from a near surface region of the boronized film because the implantation depth is limited in a few nano-meters. In the second H_2 discharge, hydrogen atoms can be absorbed instantaneously in the evacuated surface region until the saturation, and then, slowly absorbed due to the diffusion of implanted H atoms from surface into the film. The number of instantaneously absorbed H atoms (absorbed in near surface region) were, however, clearly larger than desorbed one. The He bombardment might cause not only desorption but also recoil implantation of H atoms into the film to reduce H density of the near surface region. The hydrogen accumulation during the alternate discharge of H_2 and He may be caused by a combination effect of the diffusion and the recoil implantation. It should be noted that the accuracy of the integration in Fig.5 is not good enough to compare the accumulation rate quantitatively with that of long-time H_2 discharge, which means that the difference of ion-impact effect between H_2^+ and He^+ is not clear yet.

5. SUMMARY

Hydrogen retention in the boron films during glow discharges was estimated from the pressure drop during the H_2 glow discharge. Hydrogen atoms of 1.9×10^{17} atoms/cm^2 were absorbed in the discharge of 1 hour . The hydrogen atoms were continuously absorbed for 3 hours, and the retention became 2.6×10^{17} atoms/cm^2 at 3 hour. This continuous absorption may be caused due to the diffusion of hydrogen atoms into the film.

Hydrogen atoms of 0.2×10^{17} atoms/cm^2 were desorbed by He glow discharge of 15 minutes. This corresponds to 10% of absorbed H atoms. In the second H_2 discharge after the He discharge, hydrogen atoms were absorbed instantaneously until the near surface region was saturated and slowly absorbed after that, via. diffusion. The absorbed H atoms in the second H_2 discharge were larger than the desorbed H atoms in the first He discharge. Repetition of alternate H_2 and He discharges results in H accumulation in the films.

Most of the H atoms absorbed in the films were desorbed by thermal desorption experiment up to 500°C in every case. This gives another evidence of the hydrogen accumulation during the long time H_2 discharge and repetition of alternate H_2 and He discharges.

REFERENCES

[1] J. Winter et al., J. Nucl. Mater., **162-164,** 713 (1989).

[2] H.F. Dylla et al., J. Nucl. Mater., **176-177,** 337 (1990).

[3] G.L. Jackson et al., J. Nucl. Mater., **196-198,** 236 (1992).

[4] H. Yamada et al., Jpn. J. Appl. Phys., **33,** L1638 (1994).

[5] U. Schneider et al. J. Nucl. Mater., **176-177,** 350 (1990).

[6] M. Saidoh et al., Jpn, J. Appl. Phys, **32,** 3276 (1993).

[7]S. Higashijima et al., J. Nucl. Mater., **220-222,** 375 (1995).

[8]M. Yamage, T. Ejima, H. Toyoda, and H. Sugai, J. Nucl. Mater., **196-198,** 618 (1992).

[9]N. Noda et al., J. Nucl. Mater., **220-222,** 623 (1995).

[10]N. Noda, In *Contribution to high-temperature plasma physics*, p 21. Akademie Verlarg, Beriln (1994).

FIGURE CAPTIONS

Fig.1. Time evolution of total pressure during the discharge in hydrogen after the thermal desorption of a boron coated surface. Discharge condition is as follows, pressure : 0.02 Torr, discharge current : 0.2A, and discharge voltage : 500V. Number of absorbed H atoms was calculated from the trace.

Fig.2. Time dependence of the hydrogen pressure (solid line) and temperature of the liner (dotted line) when the thermal desorption up to 500°C was carried out after the H_2 discharge for 1 hour.

Fig.3. Comparison of desorbed and absorbed number of hydrogen atoms in the case of (a) a discharge in H for 1 hour and (b) a discharge in H for 3 hour, followed by thermal desorption up to 500°C.

Fig.4. Pressure difference with respect to the initial value ($|\Delta P|$) is plotted in the cases of first, second H_2 (a,c) and the He (b) discharges.

Fig.5. The retained H atoms in the wall against time when the alternate H_2 and He discharge are repeated 6 times. Hydrogen atoms were accumulated in the film by the repetition.

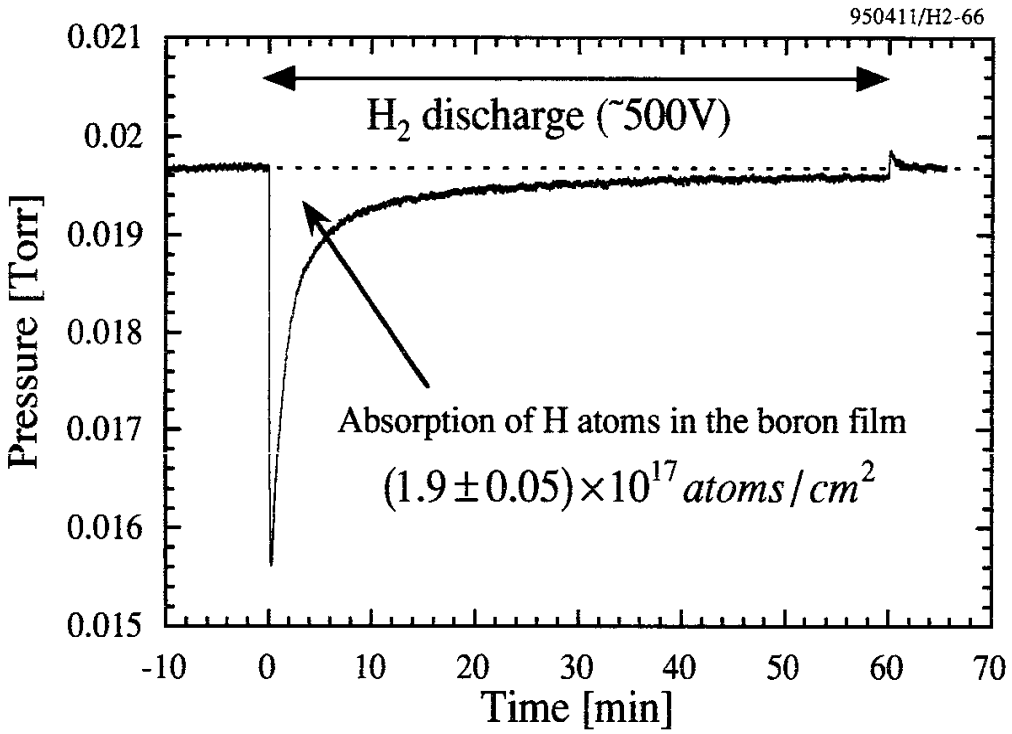

Fig. 1. K. Tsuzuki et al.

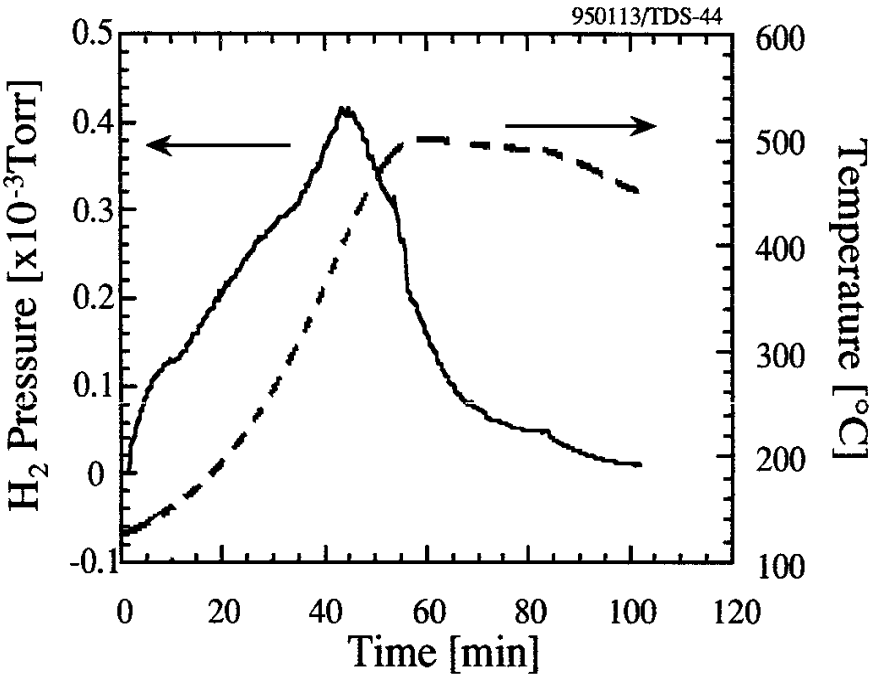

Fig. 2 K. Tsuzuki et al.

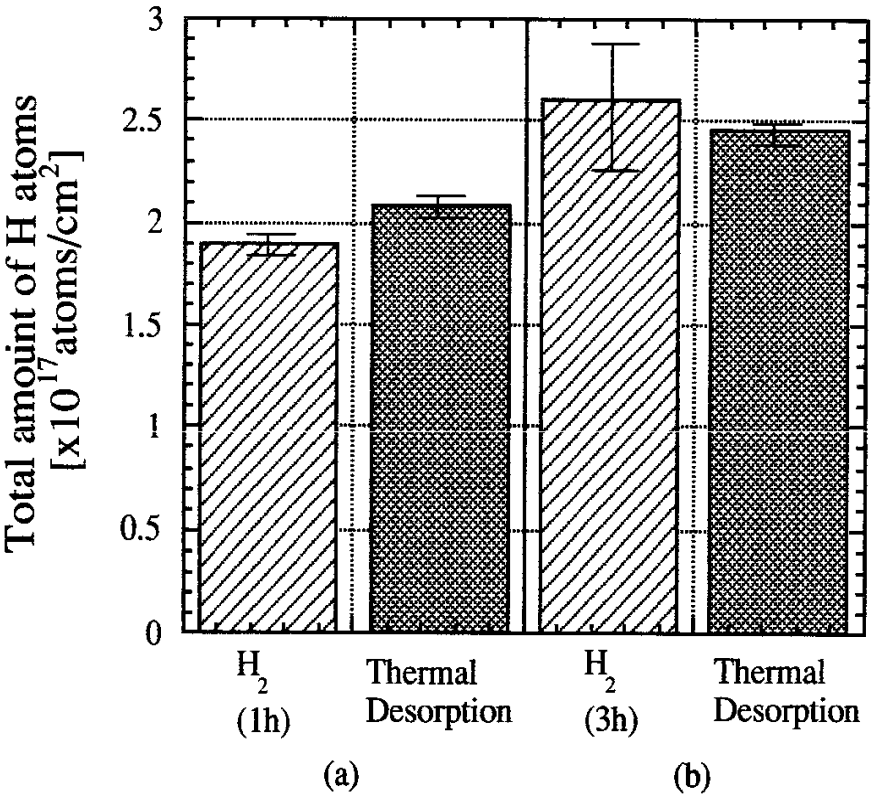

Fig. 3 K. Tsuzuki et. al.

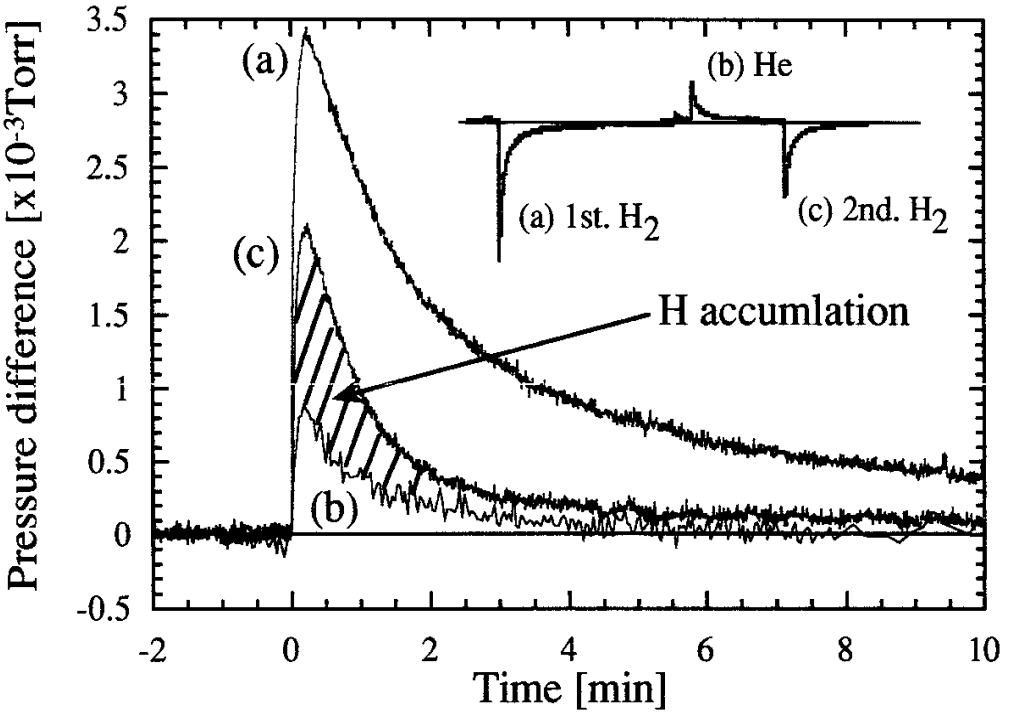

Fig. 4 K. Tsuzuki et al.

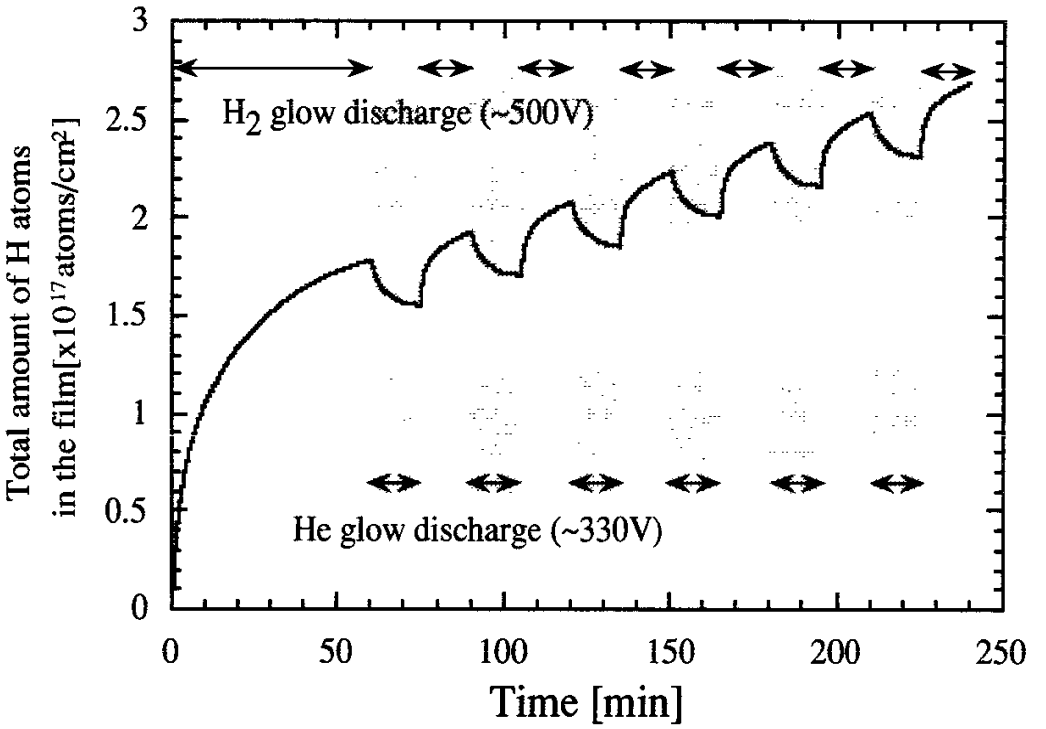

Fig. 5 K. Tsuzuki et al.

Recent Issues of NIFS Series

NIFS-326 I. Viniar and S. Sudo,
New Pellet Production and Acceleration Technologies for High Speed Pellet Injection System "HIPEL" in Large Helical Device; Dec. 1994

NIFS-327 Y. Hamada, A. Nishizawa, Y. Kawasumi, K. Kawahata, K. Itoh, A. Ejiri, K. Toi, K. Narihara, K. Sato, T. Seki, H. Iguchi, A. Fujisawa, K. Adachi, S. Hidekuma, S. Hirokura, K. Ida, M. Kojima, J. Koong, R. Kumazawa, H. Kuramoto, R. Liang, T. Minami, H. Sakakita, M. Sasao, K.N. Sato, T. Tsuzuki, J. Xu, I. Yamada, T. Watari,
Fast Potential Change in Sawteeth in JIPP T-IIU Tokamak Plasmas; Dec. 1994

NIFS-328 V.D. Pustovitov,
Effect of Satellite Helical Harmonics on the Stellarator Configuration; Dec. 1994

NIFS-329 K. Itoh, S-I. Itoh and A. Fukuyama,
A Model of Sawtooth Based on the Transport Catastrophe; Dec. 1994

NIFS-330 K. Nagasaki, A. Ejiri,
Launching Conditions for Electron Cyclotron Heating in a Sheared Magnetic Field; Jan. 1995

NIFS-331 T.H. Watanabe, Y. Todo, R. Horiuchi, K. Watanabe, T. Sato,
An Advanced Electrostatic Particle Simulation Algorithm for Implicit Time Integration; Jan. 1995

NIFS-332 N. Bekki and T. Karakisawa,
Bifurcations from Periodic Solution in a Simplified Model of Two-dimensional Magnetoconvection; Jan. 1995

NIFS-333 K. Itoh, S.-I. Itoh, M. Yagi, A. Fukuyama,
Theory of Anomalous Transport in Reverse Field Pinch; Jan. 1995

NIFS-334 K. Nagasaki, A. Isayama and A. Ejiri
Application of Grating Polarizer to 106.4GHz ECH System on Heliotron-E; Jan. 1995

NIFS-335 H. Takamaru, T. Sato, R. Horiuchi, K. Watanabe and Complexity Simulation Group,
A Self-Consistent Open Boundary Model for Particle Simulation in Plasmas; Feb. 1995

NIFS-336 B.B. Kadomtsev,
Quantum Telegragh : is it possible?; Feb. 1995

NIFS-337 B.B.Kadomtsev,

Ball Lightning as Self-Organization Phenomenon; Feb. 1995

NIFS-338 Y. Takeiri, A. Ando, O. Kaneko, Y. Oka, K. Tsumori, R. Akiyama, E. Asano, T. Kawamoto, M. Tanaka and T. Kuroda,
High-Energy Acceleration of an Intense Negative Ion Beam; Feb. 1995

NIFS-339 K. Toi, T. Morisaki, S. Sakakibara, S. Ohdachi, T.Minami, S. Morita, H. Yamada, K. Tanaka, K. Ida, S. Okamura, A. Ejiri, H. Iguchi, K. Nishimura, K. Matsuoka, A. Ando, J. Xu, I. Yamada, K. Narihara, R. Akiyama, H. Idei, S. Kubo, T. Ozaki, C. Takahashi, K. Tsumori,
H-Mode Study in CHS; Feb. 1995

NIFS-340 T. Okada and H. Tazawa,
Filamentation Instability in a Light Ion Beam-plasma System with External Magnetic Field; Feb. 1995

NIFS-341 T. Watanbe, G. Gnudi,
A New Algorithm for Differential-Algebraic Equations Based on HIDM; Feb. 13, 1995

NIFS-342 Y. Nejoh,
New Stationary Solutions of the Nonlinear Drift Wave Equation; Feb. 1995

NIFS-343 A. Ejiri, S. Sakakibara and K. Kawahata,
Signal Based Mixing Analysis for the Magnetohydrodynamic Mode Reconstruction from Homodyne Microwave Reflectometry; Mar.. 1995

NIFS-344 B.B.Kadomtsev, K. Itoh, S.-I. Itoh
Fast Change in Core Transport after L-H Transition; Mar. 1995

NIFS-345 W.X. Wang, M. Okamoto, N. Nakajima and S. Murakami,
An Accurate Nonlinear Monte Carlo Collision Operator; Mar. 1995

NIFS-346 S. Sasaki, S. Takamura, S. Masuzaki, S. Watanabe, T. Kato, K. Kadota,
Helium I Line Intensity Ratios in a Plasma for the Diagnostics of Fusion Edge Plasmas; Mar. 1995

NIFS-347 M. Osakabe,
Measurement of Neutron Energy on D-T Fusion Plasma Experiments; Apr. 1995

NIFS-348 M. Sita Janaki, M.R. Gupta and Brahmananda Dasgupta,
Adiabatic Electron Acceleration in a Cnoidal Wave; Apr. 1995

NIFS-349 J. Xu, K. Ida and J. Fujita,
A Note for Pitch Angle Measurement of Magnetic Field in a Toroidal Plasma Using Motional Stark Effect; Apr. 1995

NIFS-350 J. Uramoto,
Characteristics for Metal Plate Penetration of a Low Energy Negative Muonlike or Pionlike Particle Beam: Apr. 1995

NIFS-351 J. Uramoto,
An Estimation of Life Time for A Low Energy Negative Pionlike Particle Beam: Apr. 1995

NIFS-352 A. Taniike,
Energy Loss Mechanism of a Gold Ion Beam on a Tandem Acceleration System: May 1995

NIFS-353 A. Nishizawa, Y. Hamada, Y. Kawasumi and H. Iguchi,
Increase of Lifetime of Thallium Zeolite Ion Source for Single-Ended Accelerator: May 1995

NIFS-354 S. Murakami, N. Nakajima, S. Okamura and M. Okamoto,
Orbital Aspects of Reachable β Value in NBI Heated Heliotron/Torsatrons; May 1995

NIFS-355 H. Sugama and W. Horton,
Neoclassical and Anomalous Transport in Axisymmetric Toroidal Plasmas with Electrostatic Turbulence; May 1995

NIFS-356 N. Ohyabu
A New Boundary Control Scheme for Simultaneous Achievement of H-mode and Radiative Cooling (SHC Boundary); May 1995

NIFS-357 Y. Hamada, K.N. Sato, H. Sakakita, A. Nishizawa, Y. Kawasumi, R. Liang, K. Kawahata, A. Ejiri, K. Toi, K. Narihara, K. Sato, T. Seki, H. Iguchi, A. Fujisawa, K. Adachi, S. Hidekuma, S. Hirokura, K. Ida, M. Kojima, J. Koong, R. Kumazawa, H. Kuramoto, T. Minami,. M. Sasao, T. Tsuzuki, J.Xu, I. Yamada, and T. Watari,
Large Potential Change Induced by Pellet Injection in JIPP T-IIU Tokamak Plasmas; May 1995

NIFS-358 M. Ida and T. Yabe,
Implicit CIP (Cubic-Interpolated Propagation) Method in One Dimension; May 1995

NIFS-359 A. Kageyama, T. Sato and The Complexity Simulation Group,
Computer Has Solved A Historical Puzzle: Generation of Earth's Dipole Field; June 1995

NIFS-360 K. Itoh, S.-I. Itoh, M. Yagi and A. Fukuyama,
Dynamic Structure in Self-Sustained Turbulence; June 1995

NIFS-361 K. Kamada, H. Kinoshita and H. Takahashi,
Anomalous Heat Evolution of Deuteron Implanted Al on Electron

Bombardment; June 1995

NIFS-362 V.D. Pustovitov,
Suppression of Pfirsch-schlüter Current by Vertical Magnetic Field in Stellarators; June 1995

NIFS-363 A. Ida, H. Sanuki and J. Todoroki
An Extended K-dV Equation for Nonlinear Magnetosonic Wave in a Multi-Ion Plasma; June 1995

NIFS-364 H. Sugama and W. Horton
Entropy Production and Onsager Symmetry in Neoclassical Transport Processes of Toroidal Plasmas; July 1995

NIFS-365 K. Itoh, S.-I. Itoh, A. Fukuyama and M. Yagi,
On the Minimum Circulating Power of Steady State Tokamaks; July 1995

NIFS-366 K. Itoh and Sanae-I. Itoh,
The Role of Electric Field in Confinement; July 1995

NIFS-367 F. Xiao and T. Yabe,
A Rational Function Based Scheme for Solving Advection Equation; July 1995

NIFS-368 Y. Takeiri, O. Kaneko, Y. Oka, K. Tsumori, E. Asano, R. Akiyama, T. Kawamoto and T. Kuroda,
Multi-Beamlet Focusing of Intense Negative Ion Beams by Aperture Displacement Technique; Aug. 1995

NIFS-369 A. Ando, Y. Takeiri, O. Kaneko, Y. Oka, K. Tsumori, E. Asano, T. Kawamoto, R. Akiyama and T. Kuroda,
Experiments of an Intense H- Ion Beam Acceleration; Aug. 1995

NIFS-370 M. Sasao, A. Taniike, I. Nomura, M. Wada, H. Yamaoka and M. Sato,
Development of Diagnostic Beams for Alpha Particle Measurement on ITER; Aug. 1995

NIFS-371 S. Yamaguchi, J. Yamamoto and O. Motojima;
A New Cable -in conduit Conductor Magnet with Insulated Strands; Sep. 1995

NIFS-372 H. Miura,
Enstrophy Generation in a Shock-Dominated Turbulence; Sep. 1995

NIFS-373 M. Natsir, A. Sagara, K. Tsuzuki, B. Tsuchiya, Y. Hasegawa, O. Motojima,
Control of Discharge Conditions to Reduce Hydrogen Content in Low Z Films Produced with DC Glow; Sep. 1995